International Journal of Control, Automation and Systems VV(X) (YYYY) 1-8
http://dx.doi.org/10.1007/s12555-xxx-xxxx-x
ISSN:1598-6446 eISSN:2005-4092
http://www.springer.com/12555

Control allocation for double-ended ferries with full-scale experimental results

Tobias R. Torben, Astrid H. Brodtkorb, Asgeir J. Sørensen

Abstract: A novel control allocation algorithm for double-ended ferries with symmetrical thruster configuration is proposed. The allocation problem is formulated using the extended thrust representation, resulting in a four dimensional constrained optimization problem. Using the thrust configuration constraint, the optimization problem is reduced to a scalar bounded optimization problem, for which there exists fast solvers. We propose a cost function and bounds such that the allocation algorithm supports the standard way of performing manual thruster control on ferries. The real-time performance of the proposed algorithm is demonstrated in a simulation study, and in full-scale experiments.

Keywords: Control allocation, Thrust allocation, Autonomous ferries, Nonlinear Optimization

1. INTRODUCTION

In the recent years there has been high activity related to autonomy in ferry operations, both in academia and in the industry [1, 8, 10]. Due to the relatively low mission complexity, ferry operations make a good candidate for piloting the transition towards increased autonomy in ships.

Automating the navigation tasks requires new developments for high-level control. However, at the control execution level, functionality resembling a traditional dynamic positioning (DP) system must exist. The performance and robustness of the DP system is paramount for the success of the mission. For over-actuated marine vessels, control allocation is a vital part of the DP system. Improper allocation may lead to degraded control performance, lower energy efficiency, and increased wear and tear on the actuators.

In this paper, we treat control allocation for double-ended ferries with symmetrical thruster configuration. This is a standard setup for car ferries, of which there exists several hundred in Scandinavia. A ferry crossing typically consists of a high-speed transit phase and a low-speed docking phase. During docking, fully actuated control is normally necessary to meet the high-precision requirements in all weather conditions. A control allocation algorithm is thus called for. These ferries have one azimuth thruster in each end with the same orientation, as shown in Figure 2. A challenge with this configuration is that it may take considerable time to change the direction of thrust, as the turning rate of the azimuths is usually low. In particular, when a braking force is required, one thruster must turn 180 degrees. This time delay is unacceptable for high-precision maneuvers, such as docking. Also, if not treated carefully, the thruster may produce a force in the wrong direction while turning, which may have a destabilizing effect on the motion control system.

For manual thruster control, it is common to turn the front thruster 180 degrees when approaching the dock. A force can then quickly be produced in both forward and reverse direction by balancing the thrust on the two thrusters. At some ferry sites, turning the front thruster by 180° is restricted, as the thruster wake may cause erosion damage to the quay. In this case the aft thruster is turned instead. The principle is the same, however some thruster-thruster interactions may occur.

As far as the authors are aware, no previous published work exists for control allocation for double-ended ferries. However, there is a rich literature in control allocation for marine surface vessels, commonly referred to as *thrust allocation*. In-depth reviews of the literature are given in [5] and [6]. Two methods dominate the literature. The Pseudo-inverse method [13], and variations of the Quadratic Programming (QP) method [11]. The Pseudo-inverse method has an advantage in its simplicity and low computational complexity, but it yields an unconstrained solution. Also it does not support the thruster control

Tobias R. Torben*, Astrid H. Brodtkorb and Asgeir J. Sørensen are at the Department of Marine Technology, Norwegian University of Science and Technology (NTNU), Otto Nielsens vei 10, 7052 Trondheim, Norway. (e-mail: tobias.torben@ntnu.no, astrid.h.brodtkorb@ntnu.no, asgeir.sorensen@ntnu.no)
This work was supported by the Research Council of Norway through the Centres of Excellence funding scheme, project number 223254 - NTNU AMOS, and the KPN ORCAS project, project number 280655. The experimental testing was performed with funding from NTNU AMOS at the Autoferry project. Thanks to Brage Sæther for collaboration during testing.
* Corresponding author.

method described for manual thruster control above. The strength of the QP method is that it can add both equality and inequality constraints. Drawbacks include relatively high computational complexity and the fact that the original allocation problem must be linearized before it can be formulated as a QP problem.

The main scientific contribution of this paper is the development of an efficient nonlinear control allocation algorithm. The algorithm uses the thrust configuration constraint to reduce the solution space, and is able to control the thrusters in a similar manner as described for manual thruster control. The algorithm is tested in simulation and in full-scale experiments with the passenger ferry prototype milliAmpere, shown in Figure 1. The algorithm was originally developed for the NTNU Autoferry milliAmpere, and was first presented in [14]. Here it is elaborated upon with an extension for reversible thrusters and additional experimental results.

Fig. 1. The NTNU-developed, fully electric passenger ferry prototype, milliAmpere, used in the experimental testing. Photo: Kai T. Dragland

The paper is organized as follows: In Section 2 the problem formulation is described. In Section 3 the novel control allocation algorithm is presented. In Section 4 the results from the simulations and full-scale experiments are presented and discussed. Conclusions are given in Section 5.

2. PROBLEM FORMULATION

In this paper the control allocation problem for the thruster configuration shown in Figure 2 is considered. This figure also shows the definition of the symbols and directions used in this paper.

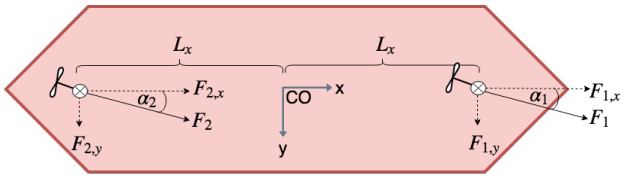

Fig. 2. Thruster configuration for double-ended ferries. F_i is the force from thruster i, with components $F_{i,x}$ and $F_{i,y}$ and angle α_i. L_x indicates the longitudonal distance from the center origin (CO) to each of the thrusters.

For marine vessels with the horizontal plane (surge, sway, yaw) as its working space, the input to the thrust allocation module is the desired body frame control action $\tau = [X, Y, N]^\top$. The output from the thrust allocation is the setpoints to the actuators. This can for instance be in form of propeller speed or pitch, engine torque or power, or rudder angle, depending on the type of actuator and the corresponding mapping of the desired force [12].

The mapping from actuator setpoints to body frame control action can be formulated as

$$\tau = B(\alpha)u \tag{1}$$

where α is a vector of unknown actuator angles and u is an unknown vector of control inputs. The matrix B is called the *thrust configuration matrix*. The objective of the control allocation problem is to find an inverse mapping, that is, determine u and α such that the resulting generalized force produced is τ. For over-actuated marine vessels, the system of (1) is under-determined, that is, there are infinitely many solutions. This gives the thrust allocation algorithm freedom to choose a combination of u and α that is optimal in some sense.

For azimuth thrusters, the dependence of B on α can be removed by considering the surge and sway components of the thrust produced from one actuator. This is referred to as the *extended thrust representation* [13]. In the case of n azimuth thrusters, (1) takes the form

$$\tau = \begin{pmatrix} 1 & 0 & \dots & 1 & 0 \\ 0 & 1 & \dots & 0 & 1 \\ -L_{1,y} & L_{1,x} & \dots & -L_{n,y} & L_{n,x} \end{pmatrix} \begin{pmatrix} F_{1,x} \\ F_{1,y} \\ \vdots \\ F_{n,x} \\ F_{n,y} \end{pmatrix} \tag{2}$$

where $L_{i,x}$ and $L_{i,y}$ are the distances from thruster i to the center origin (CO) in surge and sway directions, respectively. $F_{i,x}$ and $F_{i,y}$ are the surge and sway components of the thrust produced by thruster i. This is illustrated in Figure 2 for $n = 2$ thrusters.

From the thrust components, the thrust and azimuth angle for each thruster can be retrieved as follows:

$$T_i = \sqrt{F_{i,x}^2 + F_{i,y}^2}, \quad \alpha_i = \arctan \frac{F_{i,y}}{F_{i,x}} \tag{3}$$

3. NONLINEAR SCALAR CONTROL ALLOCATION

In this section the nonlinear scalar allocation (NSA) algorithm is presented, and guidelines for choosing the bounds on the optimization problem and the cost function are given. The section is concluded with a summary of the steps of the algorithm.

3.1. Transformation to a scalar, bounded optimization problem

When applying the extended thrust representation to the thruster configuration of Figure 2, the thrust configuration matrix, $B \in \mathbb{R}^{3\times 4}$, becomes

$$B = \begin{pmatrix} 1 & 0 & 1 & 0 \\ 0 & 1 & 0 & 1 \\ -L_{1,y} & L_{1,x} & -L_{2,y} & L_{2,x} \end{pmatrix} \tag{4}$$

By assigning the index 1 to the front thruster and 2 to the aft thruster, and exploiting the symmetry properties of double ended ferries, it is clear that $L_{1,y} = L_{2,y} = 0$ and $L_{1,x} = L_x = -L_{2,x}$. Applying this to (4) yields

$$B = \begin{pmatrix} 1 & 0 & 1 & 0 \\ 0 & 1 & 0 & 1 \\ 0 & L_x & 0 & -L_x \end{pmatrix} \tag{5}$$

A key observation here is that B is a Rank 3 matrix, whereas there are 4 unknown thrust components to be determined:

$$u = [F_{1,x}, F_{1,y}, F_{2,x}, F_{2,y}]^\top$$

Hence, there is in fact only one degree of freedom in the thrust mapping $\tau = Bu$. The main idea for the new thrust allocation algorithm is to reformulate the original optimization problem with 4 variables (7, if slack variables are used as in [7]) into a bounded scalar optimization problem in the one, free variable of the equation $\tau = Bu$.

To do this reformulation, the structure of the solution space of $\tau = Bu$ is investigated. Firstly, the augmented matrix for the linear system is set up:

$$\left(\begin{array}{c|c} B & \tau \end{array}\right) = \begin{pmatrix} 1 & 0 & 1 & 0 & X \\ 0 & 1 & 0 & 1 & Y \\ 0 & L_x & 0 & -L_x & N \end{pmatrix} \tag{6}$$

Secondly, Gaussian elimination is performed on $\left(\begin{array}{c|c} B & \tau \end{array}\right)$ until the matrix is in reduced row echolon form. This yields the equivalent linear system of equations

$$\begin{pmatrix} 1 & 0 & 1 & 0 & X \\ 0 & 1 & 0 & 0 & \frac{N+L_xY}{2L_x} \\ 0 & 0 & 0 & 1 & -\frac{N-L_xY}{2L_x} \end{pmatrix} \tag{7}$$

Written in matrix-vector form, (7) becomes

$$\begin{pmatrix} 1 & 0 & 1 & 0 \\ 0 & 1 & 0 & 0 \\ 0 & 0 & 0 & 1 \end{pmatrix} \begin{pmatrix} F_{1,x} \\ F_{1,y} \\ F_{2,x} \\ F_{2,y} \end{pmatrix} = \begin{pmatrix} X \\ \frac{N+L_xY}{2L_x} \\ -\frac{N-L_xY}{2L_x} \end{pmatrix} \tag{8}$$

Multiplying out (8) and writing out the components yields:

$$F_{1,x} + F_{2,x} = X \tag{9a}$$

$$F_{1,y} = \frac{N + L_xY}{2L_x} \tag{9b}$$

$$F_{2,y} = -\frac{N - L_xY}{2L_x} \tag{9c}$$

This shows that $F_{1,y}$ and $F_{2,y}$ are uniquely determined, whereas in (9a) there is one degree of freedom. Natural choices for the parametrization of the solution space are $F_{1,x}$ or $F_{2,x}$. $F_{1,x}$ is chosen here.

For the next stage, the idea is to search for an optimal solution by trying different choices of $F_{1,x}$. For each step of the optimization, a candidate $F_{1,x}$ is selected. From this, $F_{2,x}$, $F_{1,y}$ and $F_{2,y}$ can be calculated from (9a) - (9c) such that the thrust configuration constraint is satisfied. Now that all the thrust components are known, the thrust magnitude and angle for each thruster can be calculated from (3). Knowing the thrust magnitude and angle for each thruster, a cost function can be defined to penalize, for instance, large thrust magnitudes or large changes of azimuth angle. This shows that the value of a cost function for all possible solutions to (9a) - (9c) can be calculated by only varying $F_{1,x}$. Two great advantages are thus achieved:

1. To search for the optimal solution, one only need to solve a *scalar* optimization problem.
2. For every candidate solution, the thrust configuration constraint, $\tau = Bu$, is automatically satisfied. This removes the need for equality constraints in the optimization problem, and the optimization problem can then be reduced to a *bounded* optimization problem, where the only constraints are fixed bounds on $F_{1,x}$.

The reason why these are great advantages, is that for scalar, bounded optimization problems, there exists fast and robust nonlinear solvers. Popular alternatives include Brent's Method [3] and Golden Section Search [9]. Two example implementations are MATLABs *fminbnd* and Python SciPys *fminbound*.

3.2. Choosing the bounds in the optimization problem

There are several options for choosing the bounds on $F_{1,x}$ in the optimization problem. First of all, the bounds should ensure that the allocation algorithm does not command a greater thrust than the thrusters can deliver. To ensure that a feasible solution exists for the optimization problem, the commanded control action, $\tau = [X, Y, N]^\top$, should be saturated before entering the control allocation module. There are several options for doing this. The approach used in this paper is to first calculate $F_{1,y}$ ans $F_{2,y}$ from (9b)-(9c), and saturate them according to the max thrust. X can then be saturated based on the remaining capacity in $F_{1,x}$ and $F_{2,x}$.

If it is desirable that the front is turned 180°, as described in Section 1, this can be achieved by constraining the front thruster to only produce a negative surge force, and the aft thruster to only produce a positive surge force.

To enforce these constraints, the requirement for the front thruster is that $F_{1,x} < 0$ and $F_{1,x} > -\sqrt{T_{max}^2 - F_{1,y}^2}$, where T_{max} is the maximum thrust produced by one thruster.

Similarly, the requirement for the aft thruster is that $F_{2,x} > 0$ and $F_{2,x} < \sqrt{T_{max}^2 - F_{2,y}^2}$. Since the variable of the optimization problem is $F_{1,x}$, these constrains must be expressed in terms $F_{1,x}$. This can easily be achieved using (9a). This gives that $F_{1,x} < X$ and $F_{1,x} > X - \sqrt{T_{max}^2 - F_{2,y}^2}$.

In the end, these constraints give two upper and two lower bounds on $F_{1,x}$. The bounds used in the optimization problem are chosen to be the most restrictive of the two. This yields the bounds

$$F_{1,x}^{min} = \max(-\sqrt{T_{max}^2 - F_{1,y}^2}, X - \sqrt{T_{max}^2 - F_{2,y}^2}) \quad (10)$$

$$F_{1,x}^{max} = \min(0, X) \quad (11)$$

3.3. Choosing a cost function

In optimal control allocation algorithms, it is common to penalize the thrust magnitude, to minimize energy consumption, and to penalize the change in thrust magnitude and the change in azimuth angle to reduce wear and tear [5]. As noted in Section 3.1., it is possible to evaluate these costs for all possible solutions by only varying $F_{1,x}$. Note that when the azimuth angles enter the cost function, it becomes nonlinear due to (3).

If the thruster control method where the front thruster is turned 180 degrees is used, the offset from the *home angles*, $\alpha_1 = 180°$, $\alpha_2 = 0°$, can also be penalized to avoid large or sudden changes in the azimuth angle. When tuning the weights in the cost function, there is a trade-off between energy efficiency and control performance. If less weight is enforced on the angle change and deviation from home angle and more weight is enforced on the thrust usage and thrust change, the algorithm will allow the thrusters to have larger angular displacements. For a given commanded sway force or yaw moment, a lower thrust is then needed to produce it, since the thrust will have a larger lateral component. However, due to the low servo speed, this will also yield a larger delay from commanded forces to produced forces.

In manual thruster control during docking, it is also common to give both thrusters a mean thrust opposing each other. This yields even faster response from commanded to produced control action, since it removes much of the spin-up time. Of course, it will also increase the energy consumption since the thrusters are constantly counteracting each other. The control allocation algorithm can easily be extended to support this by adding a term in the cost function which penalizes deviations from a prescribed mean thrust.

Using all the ideas introduced in this section, the cost function can take the form

$$\begin{aligned} C(F_{1,x}, \tau, \alpha^-, T^-) = {} & w_T \|T\|^2 + w_{\Delta T} \|\Delta T\|^2 \\ & + w_{\delta T} \|\delta T\|^2 + w_{\delta\alpha} \|\delta\alpha\|^2 + w_{\Delta\alpha} \|\Delta\alpha\|^2 \end{aligned} \quad (12)$$

where $\alpha^-, T^- \in \mathbb{R}^2$ are the azimuth angles and thrust magnitudes from last time step, and $T, \alpha \in \mathbb{R}^2$ are the thrust magnitudes and azimuth angles found from (3). $F_{2,x}$ is found from (9a). $\Delta\alpha \in \mathbb{R}^2$ are the shortest angle paths from α^- to α, $\delta\alpha \in \mathbb{R}^2$ are the shortest angle paths from α to the home angles. $\Delta T \in \mathbb{R}^2$ are the changes in thrust magnitude from last time step, and $\delta T \in \mathbb{R}^2$ are the deviations from the mean thrusts. $w_T, w_{\Delta T}, w_{\delta T}, w_{\Delta\alpha}, w_{\delta\alpha} \in \mathbb{R}_{\geq 0}$ are the corresponding weights.

Collecting all the penalized variables in a vector $z = [T, \Delta T, \delta T, \delta\alpha, \Delta\alpha]^\top \in \mathbb{R}^{10}$, the cost function can be written more familiarly as a quadratic form:

$$C(z) = z^\top Q z \quad (13)$$

where $Q \in \mathbb{R}^{10\times 10}$ is a positive semi-definite diagonal matrix of weights.

3.4. Thrusters with reversible thrust

The nonlinear scalar control allocation algorithm can easily be modified to support thrusters which can reverse the thrust. In this case, the thusters do not need to turn 180 degrees to produce a braking force, and it is therefore not necessary to constrain the front thruster to only produce a negative force, and the aft thruster to produce a positive force. The constraints of (10)-(11) are thus modified to

$$F_{1,x}^{min} = \max(-\sqrt{T_{max}^2 - F_{1,y}^2}, X - \sqrt{T_{max}^2 - F_{2,y}^2}) \quad (14)$$

$$F_{1,x}^{max} = \min(\sqrt{T_{max}^2 - F_{1,y}^2}, X + \sqrt{T_{max}^2 - F_{2,y}^2}) \quad (15)$$

The solution of the optimization problem only gives the surge and sway components of the thrust for each thruster. However, when the thrusters can reverse the thurst, a given combination of $F_{i,x}$ and $F_{i,y}$ can be produced in two different ways, by reversing the thrust and turning the azimuth by 180 degrees. To find the optimal solution in this case, the optimization problem must be solved four times, with the following configurations:

- Forward thrust on both thrusters
- Forward thrust on front thruster, reversed thrust on aft thruster
- Reversed thrust on front thruster, forward thrust on aft thruster
- Reversed thrust on both thursters

The solution with minimum cost of the four is chosen. Because most thrusters are less efficient in reverse, a term can be added to the cost function to penalize reverse thrusting. A solution with reversed thrust can still be favourable, because it may lead to significantly lower change in azimuth angle, and thus less control action delay.

3.5. Summary of the control allocation algorithm

To do one iteration of the nonlinear scalar allocation algorithm, the following steps must be performed:

1. Input the desired control action, τ, and the thrust magnitudes and angles from last time step. Saturate the desired control action to ensure that a feasible solution exists.
2. Set bounds on $F_{1,x}$ using, for instance, (10)-(11) or (14)-(15).
3. Calculate $F_{1,y}$ and $F_{2,y}$ from (9b) and (9c).
4. Formulate a cost function to minimize, for instance based on (13).
5. Solve a nonlinear bounded scalar optimization problem where $F_{1,x}$ is the free variable and $F_{1,y}$, $F_{2,y}$, τ are constant parameters.
6. Calculate $F_{2,x}$ from (9a).
7. Calculate the thrust magnitude and azimuth angle setpoints from (3).

4. RESULTS AND DISCUSSION

To evaluate the performance of the novel control allocation algorithm, simulations and full-scale experiments are conducted. Simulations have the advantage that the produced thrust is known, and we can therefore compare the commanded and produced thrust. In experimental testing, the produced thrust is usually not known. Instead, the DP performance of the ferry when using the nonlinear scalar control allocation algorithm is evaluated, since good DP performance relies on good control allocation.

4.1. Simulation setup, results and discussion

In the simulation study, a simplified model for an azimuth thruster, which can not reverse the thrust, is used. The thruster dynamics are modelled as a saturated first order system:

$$\dot{T} = \frac{1}{\theta}(T_c - T) \quad (16a)$$

$$T = \max(0, \min(T_{max}, T)) \quad (16b)$$

where T_c is the commanded thrust, T is the actual thrust, T_{max} is the maximal thrust and θ is the thrust time constant.

The closed-loop azimuth servo is modelled as a proportional controller from angle offset to servo speed with saturation on the maximal servo speed. The dynamics of the servo is neglected, that is, the actual servo speed is assumed equal to the commanded servo speed.

$$\dot{\alpha} = r \quad (17a)$$

$$r = \max(-r_{max}, \min(r_{max}, -K_p(\alpha - \alpha_c))) \quad (17b)$$

where α is the actual azimuth angle, α_c is the commanded azimuth angle, r is the servo speed, r_{max} is the maximal servo speed and K_p is the proportional gain.

The commanded control action is generated stochastically from discrete first-order Gauss-Markov processes [4]. The parameters of the stochastic processes are given in Table 1. The commanded control action has some noise, which is realistic for a signal from a DP controller.

The implementation of the control allocation algorithm uses all the terms from (13). The parameters are given in Table 1. For comparison, the Pseudo-inverse and QP methods are tested under the same conditions. The implementation of the QP method is that of [5], not including the singularity avoidance term.

Figure 3 shows the commanded generalized force, τ together with the actual produced generalized force, Bu, from the nonlinear scalar allocation algorithm. The results show good tracking in all degrees of freedom.

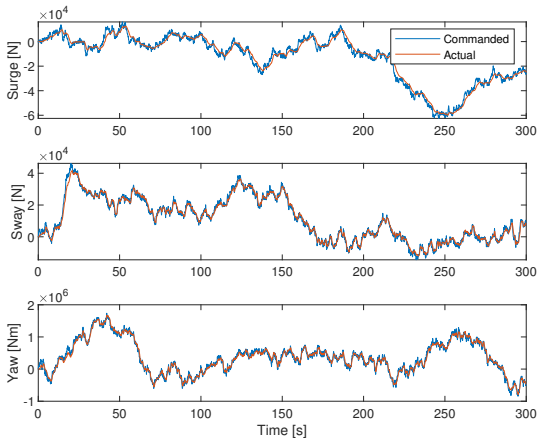

Fig. 3. Commanded and produced forces and moments for the nonlinear scalar control allocation algorithm.

Figure 4 shows the corresponding azimuth angles. The plot shows that both thrusters work in angles of $\pm 30°$ about their home angles. There is good compliance between commanded and actual azimuth angles, indicating that the allocation generates feasible references for the azimuth servos.

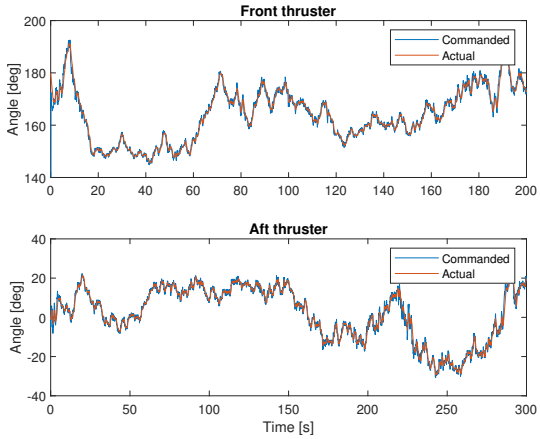

Fig. 4. Azimuth angles when using the nonlinear scalar control allocation algorithm.

Figure 5 shows the cumulative error between commanded and actual produced generalized force for the three allocation methods; Pseudo-inverse, QP, and the nonlinear scalar allocation (NSA) algorithm proposed here. The figure indicates better performance for the nonlinear scalar allocation algorithm, although this can not be claimed on this basis alone, since there is a possibility of sub-optimal tuning for the QP method. It is believed that the main reason for the improved performance is due to penalizing large angular displacements. As discussed in Section 3.3. this gives less delay in the control action and thus tighter tracking and less accumulated error. As expected, this comes at the cost of higher thrust usage. In these simulations, the mean thrust was $40.0kN$ for the NSA method and $16.2kN$ for the QP method. The trade-off between performance and thrust usage is largely determined by the weight on deviation from home angles in the cost function. It should also be mentioned that an advantage of the QP method compared to the NSA method is better handling in the case that the commanded control action is greater than the propulsion system can produce because it can include slack variables in the optimization.

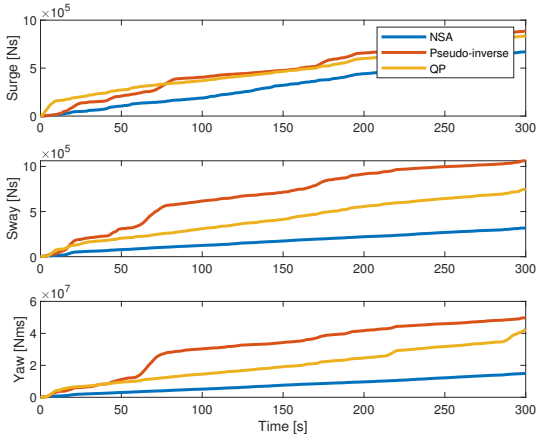

Fig. 5. Cumulative error for between commanded and produced generalized force for NSA, Pseudo-inverse and QP

The computational complexity of the QP method and the nonlinear scalar allocation algorithm are also compared. In the comparison, the MATLAB *fminbnd* solver was used for the nonlinear scalar algorithm and the MATLAB *quadprog* solver was used for the QP method. Figure 6 shows histograms of elapsed time for one iteration. The nonlinear scalar allocation algorithm is, on average, 37.8 times faster. Also, it has a more narrow distribution. This is beneficial for robustness and predictability in a real-time control system, which is of particular importance in autonomous vessels.

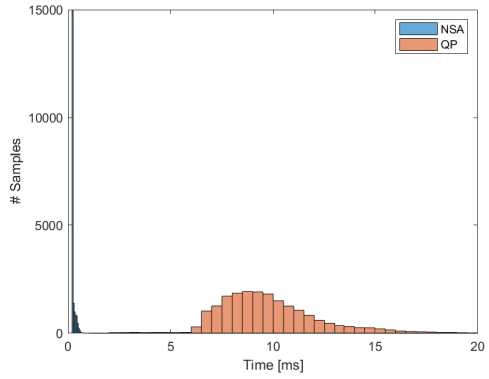

Fig. 6. Histogram of elapsed time for one iteration of NSA and QP for 20000 samples.

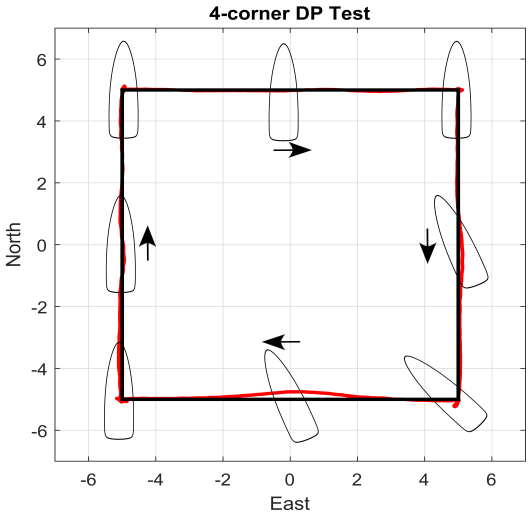

Fig. 7. Ferry trajectory from 4-corner DP test

4.2. Full-scale experimental setup, results and discussion

The experimental tests were conducted with the passenger ferry prototype milliAmpere. A maneuvering model with with hydrodynamic and rigid body data of this vessel can be found in [2]. The thrusters on this ferry can reverse the thrust, and the modifications presented in Section 3.4. was therefore used. We performed the commonly used 4-corner maneuver to evaluate the performance. The sides of the box are 10 meters, and the time used for one set-point change is about 40 seconds. Between the each set-point change, the ferry was performing stationkeeping for several minutes. In this way both the transient and stationkeeping DP performance was tested. The ferry starts in the lower-left corner and moves with the direction of the arrows. The maneuvers are becoming gradually more complex, as there is increasing coupling between the different degrees of freedom for each side of the square. The position and heading was obtained by Dual RTK GNSS, providing centimeter-level accuracy. The test was performed in calm conditions.

Figure 7 shows the trajectory for the 4-corner DP test. The figure shows good DP performance both in the transient and stationkeeping phases. As expected, there are more deviations in the third and fourth maneuvers. This is likely due to coupling between the degrees of freedom and nonlinear effects such a vortex shedding. However, compared to other 4-corner DP test results, these results are considered good.

Figure 8 shows ferry's the position and heading together with their respective references. Again, the results show good tracking. Some minor oscillations in the heading can be observed. The ferry has a flat keel, and therefore very little yaw damping. This is believed to be the reason for the heading oscillations.

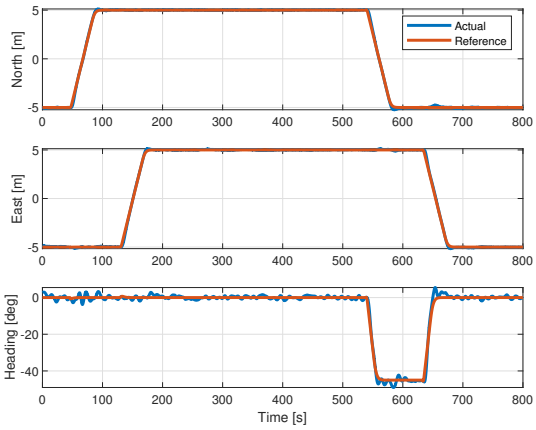

Fig. 8. Reference tracking from 4-corner DP test. Reference in red and actual in blue.

DP performance is highly dependent on the performance of the control allocation. These results therefore give increased confidence for the feasibility of the novel control allocation algorithm for use in real-time DP control systems.

5. CONCLUSION

A novel control allocation algorithm for double-ended ferries with symmetrical thruster configuration was pre-

sented. The algorithm reduces the dimension of solution space using the thrust configuration constraint, yielding a computationally efficient nonlinear optimization problem. Simulations and full-scale experimental results indicate promising real-time performance for use in a DP system.

Table 1. Parameters for simulations

Description	Value
Thrust time constant	$2.0s$
Max thrust	$200kN$
Max servo speed	$10\frac{deg}{s}$
Servo proportional gain	$3.0\frac{1}{s}$
Distance from thruster to vessel center	$50m$
Mean thrust	$50kN$
Weight on angle change	10
Weight on thrust usage	0.1
Weight on thrust change	0.1
Weight on deviation from home angle	3
Weight on deviation from mean thrust	0.1
Gauss-Markov time constant	$200s$
Gauss-Markov sample time	$0.1s$
Gauss-Markov force standard deviation	$40kN$
Gauss-Markov torque standard deviation	$300kNm$

REFERENCES

[1] Bitar, G.I. (2017). *Towards the Development of Autonomous Ferries*. Master thesis, Department of Engineering Cybernetics. Norwegian University of Science and Technology (NTNU), Trondheim.

[2] Pedersen, A.P. (2019). *Optimization Based System Identification for the milliAmpere Ferry*. Master thesis, Department of Engineering Cybernetics. Norwegian University of Science and Technology (NTNU), Trondheim.

[3] Brent, R.P. (1971). An algorithm with guaranteed convergence for finding a zero of a function. *The Computer Journal*, 14(4), 422–425.

[4] Fossen, T.I. (2011). *Handbook of Marine Craft Hydrodynamics and Motion Control*. Wiley.

[5] Fossen, T.I. and Johansen, T.A. (2006). A survey of control allocation methods for ships and underwater vehicles. *14th Mediterranean Conference on Control and Automation, MED'06*, 1–6.

[6] Johansen, T.A. and Fossen, T.I. (2013). Control allocation - A survey. *Automatica*, 49(5), 1087–1103.

[7] Johansen, T.A., Fossen, T.I., and Berge, S.P. (2004). Constrained Nonlinear Control Allocation With Singularity Avoidance Using Sequential Quadratic Programming. *IEEE Transactions on Control Systems Technology*, 12(1), 211–216.

[8] Kongsberg Maritime (2018). Teknologi til fremtidens ferger - Kongsberg Gruppen. URL `https://www.kongsberg.com/nb-no/kog/news/2018/april/teknologitilfremtidensferger/`.

[9] Press, W.H., Teukolsky, S.A., Flannery, B., and Teukolsky, S. (1992). *Numerical Recipes in C*.

[10] Rolls-Royce Marine (2018). Press releases - Rolls-Royce and Finferries demonstrate world's first Fully Autonomous Ferry –Rolls-Royce. URL `https://www.rolls-royce.com/media/press-releases/2018/03-12-2018-rr-and-finferries-demonstrate-worlds-first-fully-autonomous-ferry.aspx`.

[11] Ruth, E. (2008). *Propulsion control and thrust allocation on marine vessels*. Ph.D. thesis, NTNU.

[12] Smogeli, Ø., Ruth, E., and Sørensen, A.J. (2005). Experimental validation of power and torque thruster control. *Proceedings of the 20th IEEE International Symposium on Intelligent Control, ISIC '05 and the 13th Mediterranean Conference on Control and Automation, MED '05*, 2005, 1506–1511.

[13] Sørdalen, O.J. (1997). Optimal thrust allocation for marine vessels. *Control Engineering Practice*, 5(9), 1223–1231.

[14] Torben, T.R. (2018). *Control allocation for double-ended ferries with full-scale experimental results*. *12th Control Applications for Marine Systems, CAMS 2019*

Tobias R. Torben received his M.Sc. degree in Marine Technology from NTNU in 2019, specializing in marine cybernetics. He is currently pursuing a Ph.D. in Marine Technology at NTNU. His research interests include simulation-based verification, formal methods and risk-aware control design, with applications to autonomous surface vessels.

Astrid H. Brodtkorb received her M.Sc. degree in Marine Technology at the Norwegian University of Science and Technology (NTNU) in Trondheim in 2014. She received her Ph.D. degree in Marine Control Systems at the Norwegian Centre of Excellence Autonomous Marine Operations and Systems (NTNU AMOS) in 2017. Her main research interests are hybrid control theory, observers, and sea state estimation applied to dynamic positioning (DP) systems for marine vessels.

Asgeir J. Sørensen obtained M.Sc. degree in Marine Tech- nology in 1988 at NTNU, and Ph.D. degree in Engineering Cybernetics at NTNU in 1993. Sørensen has more than 15 years of industrial experience from ABB and Marine Cybernetics (DNV GL). Since 1999 Sørensen has held the position of Professor of Marine Control Systems at the Department of Marine Technology, NTNU. He is currently acting as key scientist and the Director of the Centre for Autonomous Marine Operations and Systems (NTNU AMOS).